

See discussions, stats, and author profiles for this publication at: <https://www.researchgate.net/publication/279098723>

Dynamics of interfacial charge-transfer reactions in semiconductor dispersions. Reduction of cobaltoceniumdicarboxylate in colloidal TiO₂

ARTICLE *in* INORGANIC CHEMISTRY · JANUARY 1985

Impact Factor: 4.76

CITATIONS

25

READS

15

3 AUTHORS, INCLUDING:



Jacques-E. Moser

École Polytechnique Fédérale de Lausanne

170 PUBLICATIONS 16,413 CITATIONS

SEE PROFILE

Table III. Atomic Parameters

atom	orbital	H_{ii} , eV	exponent
O	2s	-26.0	2.275
	2p	-16.0	2.275
Si	3s	-17.3	1.383
	3p	-9.2	1.383
Ti	4s	-8.97	1.50
	4p	-5.44	1.50
Fe	3d ^a	-10.81	4.55 (0.4391), 1.60 (0.7397)
	4s	-10.97	1.75
	4p	-7.44	1.75
	3d ^a	-12.81	5.35 (0.5505), 2.00 (0.6260)

^a Double- ζ functions with coefficients in parentheses.

lations between the ligands in calculations where these interactions were retained. Indeed we described above a significant effect of the silicon-silicon repulsions in stishovite. Recently Hyde and O'Keeffe have presented^{40b} an interesting view of the existence or nonexistence of solid-state structures using these ideas.

We may extend the orbital arguments presented above past the transition-metal series to the elements of groups 13 and 14.⁴² The orbitals for example in SiH₃, which may be identified as having the correct symmetry and energy to act as acceptor orbitals after the style of 10, are the σ^* orbitals shown in 11. In phosphines (PR₃) these are the orbitals that make this ligand an excellent π acceptor when coordinated to a transition metal. For GeO₂, SnO₂ (cassiterite), and SiO₂ (stishovite), we can imagine a similar coupling of a low-lying M-O σ^* orbital at each Ge, Sn, or Si that can stabilize the planar oxygen in a similar way. Recall in this light that SnS₂ has the cadmium iodide structure. (GeS₂ and SiS₂ have structures containing four-coordinate cations.) In an analogous fashion such orbitals may stabilize the planar nitrogen atoms in Ge₃N₄ and Si₃N₄. We reserve comment on the stabilization of linear oxygen by such a mechanism for a separate publication.²

Acknowledgment. We thank the donors of the Petroleum Research Fund, administered by the American Chemical Society,

for partial support of this research. It was also supported by the National Science Foundation via NSF Grant DMR8019741. Thanks are also due to Dr. T. Hughbanks for his assistance with some of the calculations and for several useful discussions.

Appendix

All the computations were carried out by using a program employing the extended Hückel model, which may be used for both molecular and crystal calculations. (See ref 24 for a discussion of the orbital links between the energy levels of finite and infinite molecules.) It has been developed to its present state by M.-H. Whangbo, S. Wijeyesekera, M. Kertesz, C. N. Wilker, and T. Hughbanks, and the decomposition of the energy density decomposition of states shown in Figure 9 is now routine. The crystal calculations were performed for a large enough k-point set to achieve energetic self-consistency. Typically for rutile, a set of 40 points corresponding to the irreducible wedge of the primitive tetragonal Brillouin zone was used.

Ti-O distances of 1.95 Å were employed throughout, except for those systems where more than one Ti-O distance was permitted by symmetry. In such cases this value represented the average Ti-O distance. Si-O distances were analogously fixed at 1.77 Å, close to the mean distance in stishovite.¹¹ With knowledge of the u parameter, this specifies all the geometrical details for the rutile structure. Computations on the MoO₂, PtO₂, β -ReO₂, and α -PbO₂ structures employed the fractional coordinates of ref 23, 19a, 30, and 41, respectively. The orbital parameters are shown in Table III. The modified weighted Wolfsberg-Helmholz equation was used to estimate the interaction integrals.

(41) Wyckoff, R. G. W. "Crystal Structures"; Wiley: New York, 1973.

(42) In this paper the periodic group notation is in accord with recent actions by IUPAC and ACS nomenclature committees. A and B notation is eliminated because of wide confusion. Groups IA and IIA become groups 1 and 2. The d-transition elements comprise groups 3 through 12, and the p-block elements comprise groups 13 through 18. (Note that the former Roman number designation is preserved in the last digit of the new numbering: e.g., III \rightarrow 3 and 13.)

Contribution from the Institut de Chimie Physique, Ecole Polytechnique Fédérale, CH-1015 Lausanne, Switzerland

Dynamics of Interfacial Charge-Transfer Reactions in Semiconductor Dispersions. Reduction of Cobaltoceniumdicarboxylate in Colloidal TiO₂

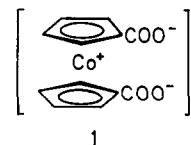
ULRICH KÖLLE,¹ JACQUES MOSER, and MICHAEL GRÄTZEL*

Received November 2, 1984

The dynamics of electron transfer from the conduction band of colloid TiO₂ solutions in water to cobaltoceniumdicarboxylate [Co(C₅H₄COO)₂]⁻ (1) were investigated by using laser photolysis to excite the semiconductor. The decay of the blue color of the electron in the TiO₂ particle as well as the formation of the 484-nm absorption of [Co(C₅H₄COO)₂]²⁻ was used to monitor the course of the reaction. At pH 10, the electron spectrum has a maximum at 780 nm and its extinction coefficient at this wavelength has been determined as 800 M⁻¹ cm⁻¹. The rate of reduction is controlled by the interfacial charge-transfer step. The unique pH effect on the rate constant can be understood in terms of simultaneous protonation of the two carboxylate groups of the reduced acceptor. In acidic solution 1 affords a drastic (up to 50-fold) enhancement of interfacial conduction band electron transfer to other acceptors such as viologens.

Introduction

In a previous communication² we have introduced cobaltoceniumdicarboxylate (1) as a new redox mediator for light energy conversion devices. Subsequent experiments showed that this electron acceptor is superior to methylviologen when used in aqueous chloroplast suspensions as a relay compound for hydrogen generation³ or in regenerative photoelectrochemical cells based



1

on p-InP semiconductor electrodes.⁴ Advantages of this mediator are its high chemical stability⁵ and relatively weak visible light absorption in both the oxidized and the reduced form. In neutral

(1) Visiting scientist from the Institut für Anorganische Chemie, Technische Hochschule, D-5100 Aachen, West Germany.

(2) Houlding, V.; Geiger, T.; Kölle, U.; Grätzel, M. *J. Chem. Soc., Chem. Commun.* 1982, 682.

(3) Cuendet, P.; Grätzel, M. *Photochem. Photobiol.* 1982, 36, 203.

(4) Geiger, T.; Nottenberg, T.; Pélaprat, M.-L. *Helv. Chim. Acta* 1982, 65, 2507.

(5) Sheats, J. E. *J. Organomet. Chem. Libr.* 1979, 7, 461.

or alkaline water/EtOH (30%) mixtures reversible one-electron reduction of **1** occurs at -0.65 V (NHE),⁶ rendering thermodynamically feasible the reduction of water to H_2 or CO_2 to formate and oxalate by cobaltocenedicarboxylate.

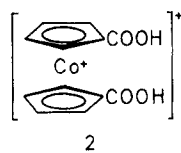
Recently, we have initiated^{7,8} laser photolysis studies with colloidal semiconductors to probe the dynamics of charge-transfer reactions at the particle/solution interphase. The transparent nature of these sols renders feasible the application of time-resolved absorption spectroscopy and thus allows for the analysis of the behavior of transient species involved in the electron-transfer event. Here, we give a detailed report on the reduction of **1** by conduction band electrons of TiO_2 particles. Furthermore, it will be shown that **1**, when adsorbed at the TiO_2 surface, can act as a molecular electron-transfer catalyst enhancing both the rate and yield of reduction of other acceptors such as viologenpropanesulfonate.

Experimental Section

Preparation and Characterization of Colloidal TiO_2 . $TiCl_4$ (Fluka puriss.) was further purified by vacuum distillation ($40^\circ C$, ca. 25 torr) until a colorless liquid was obtained. Hydrolysis in cold ($\sim 0^\circ C$) water was performed as previously described.⁹ Poly(vinyl alcohol) (PVA; Mowiol 10-98, Hoechst), pretreated by UV light to remove impurities,^{9b} was used to stabilize the colloidal TiO_2 particles. Application of transmission electron microscopy as well as quasi-elastic light-scattering techniques yielded an average particle radius of 50 Å. These aggregates consist of both amorphous phase and anatase as shown by dark-field electron microscopy and electron diffraction techniques. The point of zero ζ potential of the TiO_2 particles was determined as 4.7 by using a Rank Bros. Mark II electrophoresis instrument. Optical absorption measurements yielded an extinction coefficient of $\epsilon = 0.785 \text{ g}^{-1} \text{ L cm}^{-1}$ at $\lambda = 347 \text{ nm}$.⁹

Apparatus. Laser photolysis experiments employed a frequency-doubled JK 2000 ruby laser combined with fast-kinetic spectroscopy to detect transient species.¹⁰ Continuous illumination was carried out with a XBO 450-W Xe lamp (Osram) equipped with a 15-cm water jacket to remove IR radiation. UV/visible and near-IR absorption spectra were recorded on a Perkin-Elmer Hitachi 340 spectrophotometer. A Metrohm EA 505 polarograph operated in the differential-pulse mode was used to determine the pH dependency of the redox potential of **1** in aqueous solution. Supporting electrolyte was 0.2 M KCl, and the pH was adjusted by phosphate and borate buffers. Concentration of **1** was 10^{-3} M. The half-widths of the polarographic peaks obtained indicated reversible electron transfer under all pH conditions. Acid-base titration used an automatic system (Metrohm 636 titriprocessor).

Materials. The synthesis of cobaltoceniumdicarboxylic acid chloride (**2-Cl**) was a modified version of the procedure described by Fischer and Herberich.¹¹ To a concentrated alkaline aqueous solution of 1,1'-di-



methylcobaltocenium chloride was added excess $KMnO_4$ and the mixture agitated for 8–10 h on a boiling water bath. Excess $KMnO_4$ was reduced with SO_2 , the solution filtered from MnO_2 , and the precipitate extracted with several portions of hot water until these were nearly colorless. The combined filtrates were evaporated to dryness in a rotavap, and the residue was extracted with the minimum quantity of hot absolute methanol/acetone (1:1 v/v). On slight cooling, a small quantity of KCl precipitated, from which the solution was decanted, and on further cooling to $-60^\circ C$, the product crystallized as yellow needles.

Methylviologen dichloride (BDH) was used as supplied. Viologenpropanesulfonate was synthesized as previously described.¹² Deionized

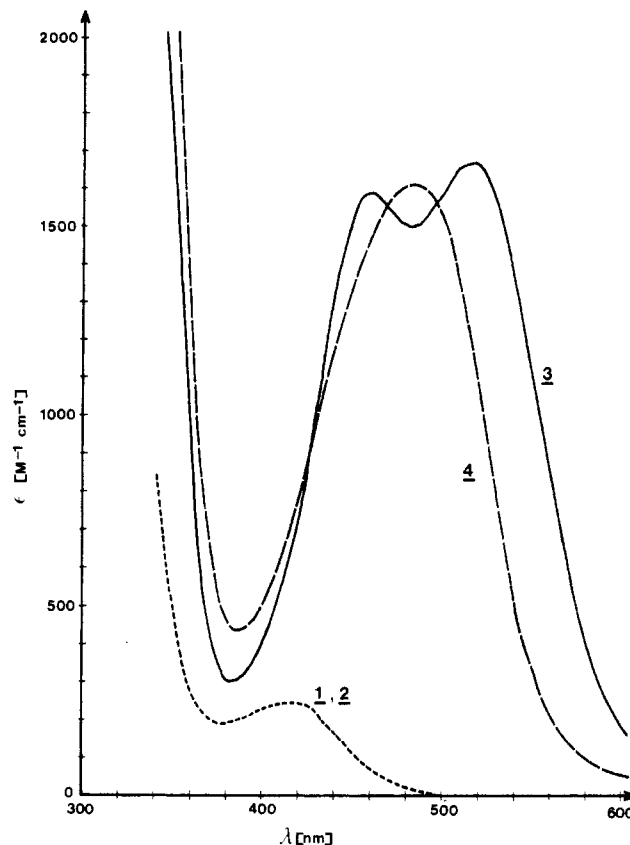
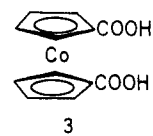


Figure 1. Absorption spectra of cobaltoceniumdicarboxylate (**1**) and its protonated form (**2**) as well as cobaltocenedicarboxylic acid (**3**) and its conjugate base (**4**) in water/ethanol mixture (2:1 v/v).

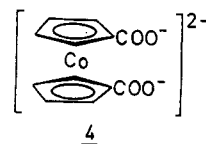
water was further purified by refluxing over $KMnO_4$ and subsequent distillation from a quartz still.

Determination of the pK Values of Cobaltocenium- and Cobaltocenedicarboxylic Acids. The titration of 40 mL of a 10^{-3} M aqueous solution of **2** with 10^{-2} M NaOH yields one equivalent point, from which one derives $pK_1 = pK_2 = 2.9$. The acid dissociation constants for the two carboxyl groups are the same and are equal to 1.3×10^{-3} . Since the reduced form of **2**, i.e. cobaltocenedicarboxylic acid (**3**), is poorly soluble



in water, experiments to determine its pK values were performed in ethanol/water mixtures. A 0.2-mmol quantity of **2** was dissolved in a mixture of 5 mL of 0.1 N NaOH and 10 mL of EtOH, and after flushing of the solution with N_2 , **2** was reduced by controlled-potential electrolysis (Hg cathode, -1.0 V, SCE). After completion of the reduction, the solution was titrated with N_2 -saturated 0.1 N HCl under N_2 .¹³ Again, only one equivalent point was found, indicating that dissociation of the two protons of **3** occurs in one step, as was observed for **2**. From the pK value, $pK_1 = pK_2 = 5.8 \pm 0.3$, one infers that reduced cobaltocenedicarboxylic acid is a considerably weaker acid than the oxidized form.

Absorption Spectra of Cobaltocenium- and Cobaltocenedicarboxylic Acids. The absorption spectrum of **1** in aqueous solution and that of **3**, as well as its conjugate base, i.e., cobaltocenedicarboxylate **4**, in



- (6) El Murr, N. *Transition Mt. Chem.* **1981**, 6, 321.
- (7) Duonghong, D.; Borgarello, E.; Grätzel, M. *J. Am. Chem. Soc.* **1981**, 103, 6547.
- (8) Duonghong, D.; Ramsden, J.; Grätzel, M. *J. Am. Chem. Soc.* **1982**, 104, 2977.
- (9) (a) Moser, J.; Grätzel, M. *J. Am. Chem. Soc.* **1983**, 105, 6547. (b) Moser, J.; Grätzel, M. *Helv. Chim. Acta* **1982**, 65, 1436.
- (10) Rothenberger, G.; Infelta, P. P.; Grätzel, M. *J. Phys. Chem.* **1979**, 83, 1871.
- (11) Fischer, E. O.; Herberich, G. E. *Chem. Ber.* **1961**, 94, 1517.

- (12) Brugger, P. A.; Grätzel, M.; Guarr, T.; McLendon, G. *J. Phys. Chem.* **1982**, 86, 944.

- (13) During titration the ratio of water to alcohol increases to reach a final proportion of 2:1.

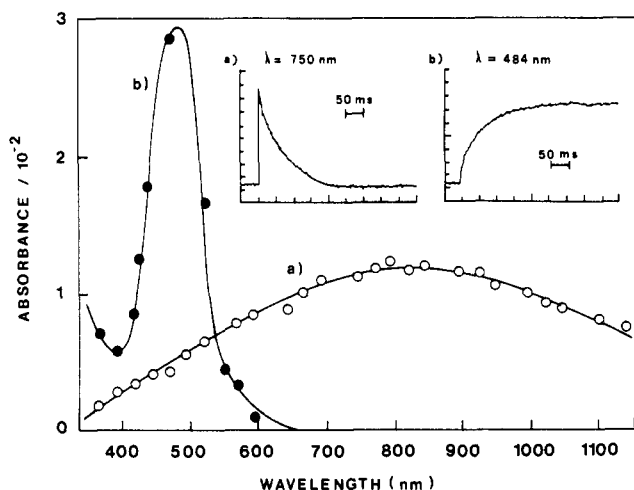


Figure 2. Transient spectra obtained from the laser photolysis of alkaline (pH 10) solutions of colloidal TiO_2 (0.5 g/L) in the presence of 5×10^{-4} M **1** (concentration of PVA is 0.5 g/L): O, spectrum $\sim 10 \mu\text{s}$ after the laser pulse; ●, spectrum 400 ms after the laser pulse. Insert shows temporal evolution of the absorbance at 750 and 484 nm.

water/ethanol mixture (2:1, v/v), are shown in Figure 1. The visible and near-UV absorption of **1** is very weak ($\lambda_{\text{max}} = 410 \text{ nm}$, $\epsilon = 240 \text{ M}^{-1} \text{ cm}^{-1}$) and by analogy with the unsubstituted cobaltocenium ion is attributed to d-d transitions.¹⁴ No change in the spectrum occurs in acidic solution upon protonation of the carboxylate groups. By contrast, the spectrum of the reduced form **4** is pH sensitive. Thus, at pH 12.5, a single maximum at 484 nm is obtained ($\epsilon_{484} = 1615 \text{ M}^{-1} \text{ cm}^{-1}$) while at pH 1.35 one observes two maxima ($\lambda = 516 \text{ nm}$, $\epsilon_{516} = 1657 \text{ M}^{-1} \text{ cm}^{-1}$ and $\lambda = 454 \text{ nm}$, $\epsilon_{454} = 1580 \text{ M}^{-1} \text{ cm}^{-1}$). These spectra are attributed to **4** and its conjugate acid **3**, respectively. Detailed spectrophotometric studies of solutions of reduced **1** as a function of pH confirmed the simultaneous two-proton dissociation from cobaltocenedicarboxylic acid (**3**) and yielded a pH value in agreement with the one derived from acid-base titration.

Acid solutions of **3** in deoxygenated mixtures of water/ethanol were found to be unstable and degraded slowly. Thus, at pH 1.35 one obtained from the decrease of the 516-nm absorbance a first-order decay law for **3** with a rate constant of $7.8 \times 10^{-5} \text{ s}^{-1}$. The decomposition leads mainly to formation of Co^{2+} ions (yield 95%, as determined by photometric analysis as the $\text{Co}(\text{SCN})_4^{2-}$ complex), re-formation of **2** accounting only for 5% of the reaction. The decay of **3** was found to be enhanced by light. No thermal degradation occurred in alkaline solution, where the deprotonated form **4** is present. However, photodecomposition of **4** was still observed under these conditions. In the calculation of the extinction coefficient for **3** in Figure 1, thermal decomposition was taken into account by extrapolating the extinction values back to the time when the solution was acidified.

Results

Figure 2 shows absorption spectra obtained from the laser photolysis of alkaline (pH 10) solutions of colloidal TiO_2 (0.5 g/L) in the presence of 5×10^{-4} M cobaltocenedicarboxylate. Inserted are two oscillograms illustrating the temporal behavior of the optical density at 750 and 484 nm. Immediately after the laser flash a species is observed exhibiting a broad absorption in the visible and IR regions with a maximum at 800 nm. The decay of this transient obeys a first-order rate law, the observed rate constant increasing linearly with the concentration of cobaltocenedicarboxylate. A second-order rate constant of $4 \times 10^4 \text{ M}^{-1} \text{ s}^{-1}$ is evaluated from the kinetic analysis performed with concentrations of **1** varying from 1×10^{-4} to $2 \times 10^{-3} \text{ M}$. The second spectrum in Figure 2 with a maximum at 484 nm was obtained 400 ms after the laser pulse. It is identical with that obtained for cobaltocenedicarboxylate (**4**) in Figure 1. Kinetic analysis of the absorption growth at 484 nm showed that it obeys the same time law as the 800-nm decay.

Continuous-photolysis experiments confirmed that **3** is the stable product from the photoreaction of colloidal TiO_2 with **1**. Thus,

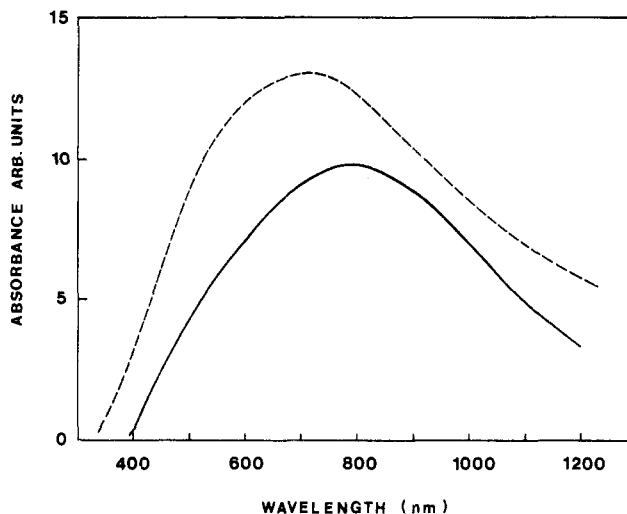


Figure 3. Optical absorption spectra of electrons in colloidal TiO_2 particles at pH 10 (solid line) and 3 (dashed line).

at pH 9.1 and experimental conditions as in Figure 2, the TiO_2 sol turns orange/red when exposed to UV light. Spectral analysis shows 50% conversion of **1** into **4** after 15-min illumination of 20 mL of deaerated colloidal TiO_2 solution by the 450-W Xe lamp.

The species with a maximum at 800 nm is observed also in the absence of **1** when alkaline colloidal TiO_2 solutions are excited with a laser pulse. It is relatively stable in deaerated sols but reacts readily with electron acceptors such as O_2 or MV^{2+} . This species is identified with the conduction band electron (e_{cb}^-) produced by bandgap excitation in the TiO_2 particle. Under continuous illumination of deoxygenated TiO_2 sols one observes the formation of a blue color¹⁵ arising from the accumulation of e_{cb}^- in the particles. This effect was quantitatively investigated in the following experiment: A colloidal solution containing 1.5 g/L TiO_2 and 1 g/L PVA was alkalized with NaOH to pH 10, degassed with Ar, and irradiated for 12 h with a Hanau Suntest lamp (6-07-004). A volume of 3.5 mL of this solution was transferred under N_2 into a 1-cm optical quartz cell and irradiated for an additional 1 h with a 450-W Xe arc lamp. This doubled the intensity of the blue color without changing the spectral characteristics. The final optical density was 0.243 at 780 nm, measured against an aerated sample of the same solution to compensate for light scattering. The absorption spectrum of the blue sol, shown in Figure 3, was found to be identical with that of the transient obtained after laser excitation of colloidal TiO_2 in Figure 2. After recording of the spectrum, 0.05 mL of a 10^{-2} M solution of **1** adjusted to pH 10 and flushed with Ar was added with a syringe. The solution turned immediately orange/red and displayed the absorption spectrum of **4**. Further addition of **1** produced no increase in the 484-nm absorption, indicating that the reaction of e_{cb}^- with **1** was complete. Since the extinction coefficient of **4** at 484 nm is known, the concentration of e_{cb}^- as well as its extinction coefficient can be readily evaluated. One obtains $[e_{\text{cb}}^-] = 2.9 \times 10^{-4} \text{ M}$, which, in view of the TiO_2 particle concentration of $9.4 \times 10^{-7} \text{ M}$ employed in this experiment, corresponds to 309 electrons stored in one particle, or a carrier density of $5.9 \times 10^{20} \text{ cm}^{-3}$. For the extinction coefficient of $e_{\text{cb}}^- (\text{TiO}_2)$ at 780 nm one obtains the value $800 \text{ M}^{-1} \text{ cm}^{-1}$.

Irradiation of colloidal TiO_2 (1 g/L) protected by PVA (1 g/L) in acidic solution (pH 3) produces also intense blue coloration resulting from the accumulation of electrons in the particles. Included in Figure 3 is the visible and near-IR absorption spectrum of a sol illuminated for ca. 14 h by the suntest lamp. The spectrum in the visible region at pH 3 is broader than that obtained at pH

(14) Weber, J.; Goursot, A.; Pénigault, E.; Ammeter, J. H.; Bachmann, J. *J. Am. Chem. Soc.* **1982**, *104*, 1491.

(15) Blue color formation was observed in our earlier study⁷ with TiO_2 sols prepared from titanium isopropoxide. The electron spectrum was somewhat different in this case. Recently, Bahnmann et al. have supported flash photolysis results with colloidal TiO_2 , where the electron spectrum had a maximum around 650 nm.¹⁹

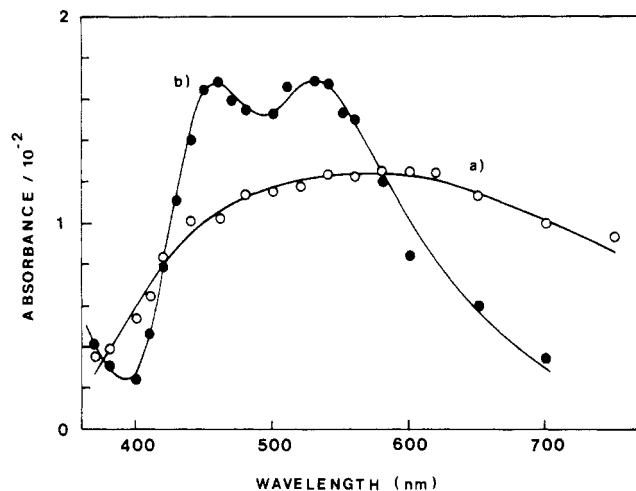


Figure 4. Transient spectra obtained from the laser photolysis of acid (pH 3) colloidal TiO_2 solutions in the presence of 2×10^{-4} M **1** (concentration of TiO_2 and PVA is 500 mg/L): (a) spectrum $\sim 10 \mu\text{s}$ after the laser pulse; (b) spectrum 2 ms after the laser pulse.

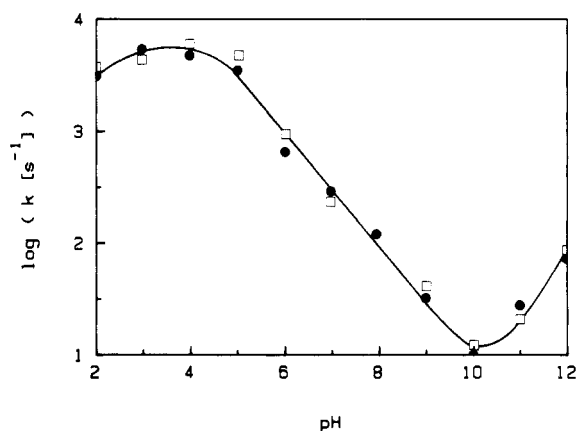


Figure 5. Effect of pH on the rate of reduction of **1** by TiO_2 conduction band electrons: (●) kinetics of 484-nm absorption growth; (□) kinetics of 750-nm absorption decay. The decadic logarithm of the pseudo-first-order rate constant obtained at 2×10^{-4} M concentration of **1** is plotted against pH. Other conditions are as in Figure 4.

10, and its maximum is shifted to 670 nm.

A similarly broad absorption is observed when the laser is used to excite the particles. Figure 4 shows transient spectra obtained with colloidal TiO_2 (0.5 g/L, protected by 0.5 g/L PVA, adjusted with HCl to pH 3) in the presence of **1** (2×10^{-4} M). Curve a corresponds to the species present immediately after the laser pulse while curve b is the spectrum of the product observed after the decay of the transient. The maximum of curve a is located around 600 nm. Due to the weak intensity and the broad nature of the transient absorption, the λ_{max} value is not very precise. Nevertheless, it is readily apparent from comparing Figures 4a and 2a that the transient spectrum is considerably broader at pH 3 than in alkaline solution and that this is due to an increased extinction in the 400–600 nm wavelength domain. Spectrum b in Figure 4 is readily identified with that of **3**, i.e. cobaltocenedicarboxylic acid.

The effect of pH on the rate of reduction of **1** by TiO_2 conduction band electrons is shown in Figure 5. Laser photolysis experiments employed 2×10^{-4} M solutions of **1** or its conjugate acid **2** together with 0.5 g/L TiO_2 protected by 0.5 g/L PVA. The transient absorption decay at 750 nm and the kinetics of cobaltocene growth were analyzed to determine the rate constant for electron transfer (k_{et}). In Figure 5 one distinguishes three domains: Between pH 2 and 4, k_{et} increases slightly with pH. In pH interval pH 5–10, k_{et} decreases by almost 3 orders of magnitude, $d \log k_{\text{et}}/d\text{pH}$ being -0.5 . This trend is inverted above pH 10, where $d \log k_{\text{et}}/d\text{pH}$ has a positive value of about 0.5.

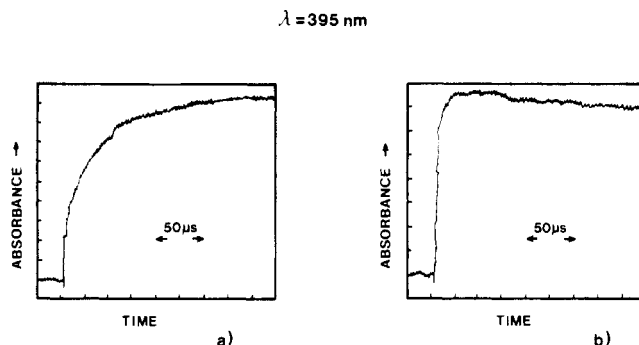
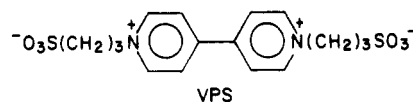


Figure 6. Oscillograms from the laser photolysis of colloidal TiO_2 (0.5 g/L) in the presence of 10^{-3} M viologenpropanesulfonate as electron acceptor, pH 3.5. No PVA protective agent was employed. Temporal evolution of the 395-nm absorption of reduced viologen is reported: (a) no $[\text{Co}(\text{C}_5\text{H}_4\text{COO})_2]^-$; (b) $[\text{Co}(\text{C}_5\text{H}_4\text{COO})_2]^- = 1 \times 10^{-5}$ M.

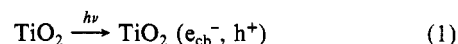
Figure 6 shows oscillograms obtained from the laser photolysis of colloidal TiO_2 (pH 3.5) in the presence of 10^{-3} M viologenpropanesulfonate (VPS) as electron acceptor. The purpose of these



experiments was to explore whether the interfacial electron transfer from the conduction band to this acceptor, which is relatively slow at pH 3.5,⁹ could be accelerated by using cobaltoceniumdicarboxylate as mediator. The TiO_2 sol was employed without PVA as protective agent. The oscilloscope traces in Figure 6 present temporal behavior of the absorbance at 395 nm, where the singly reduced acceptor, VPS^- , has a strong and characteristic absorption maximum. For ease of comparison, both traces were recorded on the same time scale. In the absence of **1** the growth of the 395-nm absorption occurs over a time period of ca. 500 μs . Detailed kinetic evaluation yielded for the reduction of VPS by conduction band electrons a pseudo-first-order rate constant of $k_{\text{et}} = (6 \pm 2) \times 10^3 \text{ s}^{-1}$. Addition of 10^{-5} M **1** drastically accelerates the electron-transfer rate and augments the yield of VPS^- formation by a factor of 3. Thus, in Figure 6b the growth of the 395-nm absorbance is completed a few microseconds after the laser pulse. The pseudo-first-order rate constant for VPS^- formation is $1.2 \times 10^5 \text{ s}^{-1}$ under these conditions, i.e. 20 times higher than in the absence of **1**. Increasing the concentration of **1** to 10^{-4} M increases the rate constant further to $3 \times 10^5 \text{ s}^{-1}$, indicating at 50-fold enhancement of the electron-transfer rate. It should be noted that this effect cannot be ascribed to a change in pH since the pH value of the solution was strictly maintained at 3.5 throughout these experiments.

Discussion

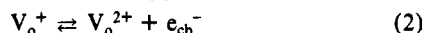
Our experimental observations are rationalized in terms of bandgap excitation of the colloidal TiO_2 particles generating electron-hole pairs:



In the presence of hole scavengers electrons accumulate in the particles under illumination, rendering the solution deep blue. The transparent character of these sols allowed for the first time quantitative evaluation of the extinction coefficient of the electron, which is $800 \text{ M}^{-1} \text{ cm}^{-1}$ at 780 nm. The charge-carrier density produced after several hours of photolysis is $6 \times 10^{20} \text{ cm}^{-3}$, which corresponds to one-tenth of the density of states available in the TiO_2 conduction band. For a freely moving conduction band electron, one would expect the extinction coefficient to increase continuously with wavelength ($\epsilon \sim \lambda^n$). Such a free carrier absorption has indeed been observed for colloidal anatase particles by Nozik et al.¹⁶ The fact that our electron spectrum exhibits

(16) We thank Dr. A. Nozik, SERI, Golden, CO, for communicating to us these results prior to publication.

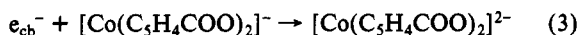
a maximum indicates that at least part of the charge carriers are trapped. From studies of thermally stimulated currents and luminescence, Gosh et al.¹⁷ concluded that there are at least eight different traps present in rutile with depth levels ranging from 0.21 to 0.87 eV. These traps have been ascribed to point defects, i.e. interstitial titanium ions and oxygen vacancies (V_o^{+}):



According to Gosh et al. such a center would have an optical ionization energy of 1.18 eV. The optical transition associated with interstitial Ti^{3+} ions in an octahedral environment is expected to be weak and to be located around 500 nm.²⁵

An interesting observation in Figures 3 and 4 is that the electron spectrum is sensitive to changes in solution pH. The maximum at pH 3 is blue shifted by about 100 nm and its intensity in the 400–600-nm region is increased when compared to that obtained at pH 10. The fact that the nature of the traps is influenced by the degree of protonation of the particles indicates that they are located close to the surface. This may be due to the small size of the particle leading to the exposure of a relatively large fraction of the TiO_2 molecules, i.e. 20%, to the aqueous phase.

In the presence of cobaltoceniumdicarboxylate one observes the reaction



The concomitant hole reaction comprises oxidation of TiO_2 surface bound hydroxide ions to hydroxyl radicals, which either dimerize to form peroxides or react with the PVA polymer employed in most experiments as a protective agent to prevent particle flocculation. The fate of the radical produced by OH or direct hole attack on PVA has been previously discussed.⁹ Most likely, they undergo dimerization and/or dismutation. Intervention of these radicals as reducing agents for **1** or **2** can be excluded on the basis of the detailed time-resolved absorption studies performed in the present investigation. The decay of the conduction band electron always followed the same time law as the formation of cobaltocenedicarboxylate, and there was no indication of a secondary reduction process involving PVA.¹⁸ This is clearly demonstrated in Figure 5, where over the whole pH domain investigated the rate constant derived from the decrease of the 750-nm electron absorption is practically identical with that obtained from the 484-nm growth of $Co(C_5H_4COO)_2^{2-}$. Furthermore, replacing PVA with another hole scavenger such as formate, had no effect on the reduction rate. It is concluded that the events observed correspond unambiguously to electron transfer from the TiO_2 particles to cobaltoceniumdicarboxylate in solution.

In Figure 5 we observed a drastic pH effect on the rate of reaction 3. In order to rationalize this finding, we apply a simple kinetic model introduced by us earlier to analyze methylviologen reduction by TiO_2 conduction band electrons.^{9,20} The overall reaction is divided up into two elementary steps comprising diffusional encounter of the TiO_2 particle with the acceptor followed by interfacial electron transfer. In Figure 5 the observed pseudo-first-order rate constant never exceeds $5 \times 10^3 s^{-1}$, which, when divided by the concentration of acceptor, gives $k_2 = 2.5 \times 10^7 M^{-1} s^{-1}$. This is far below the diffusion-controlled limit of the second-order rate constant, which for a 50-Å-radius TiO_2 particles is $5 \times 10^{10} M^{-1} s^{-1}$. Therefore, in the reaction of conduction band electrons with cobaltoceniumdicarboxylate, interfacial charge transfer is rate determining. Under these conditions the second-order rate constant is given by⁹

$$k_2 = 4\pi r^2 N_A k_{het} \quad (4)$$

(17) Gosh, A. K.; Wakim, F. G.; Addis, R. B. *Phys. Rev.* **1969**, *184*, 979.

(18) In a recent paper,¹⁹ Bahnemann et al. claim to have observed reduction of methylviologen (MV^{2+}) due to PVA radicals resulting from the reaction of $h^+(TiO_2)$ with PVA. We find at pH ≤ 4 precisely the same growth kinetics for MV^{+} in the absence and presence of PVA protective agent, which excludes such a reaction at least for the type of PVA employed in our experiments.

(19) Bahnemann, D.; Henglein, A.; Lilie, J.; Spanhel, L. *J. Phys. Chem.* **1984**, *88*, 709.

(20) Brown, G. T.; Darwent, J. R. *J. Chem. Soc., Faraday Trans. 1* **1984**, *80*, 1631.

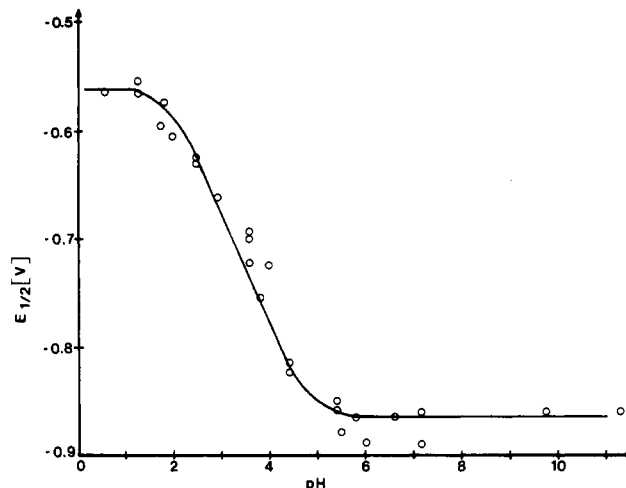


Figure 7. Polarographic half-wave potential (measured against SCE) for the reduction of **1** as a function of pH (conditions are given in Experimental Section).

where N_A is Avogadro's number and k_{het} ($cm s^{-1}$) the heterogeneous rate constant for electron transfer from TiO_2 to **1** or **2** at the surface of the particle.

The rate parameter k_{het} can be expressed by a Tafel relation:

$$k_{het} = k_{het}^0 \exp(-\alpha F \eta / RT) \quad (5)$$

where α is the electrochemical transfer coefficient and η is the overvoltage available to drive the interfacial electron transfer, defined as

$$\eta = E_{cb}(TiO_2) - E^0(A/A^-) \quad (6)$$

The conduction band potential, E_{cb} , as well as the standard redox potential of the cobaltoceniumdicarboxylate acceptor, $E^0(A/A^-)$, depends on pH. For our colloidal TiO_2 we found^{9a}

$$E_{cb}(TiO_2) = -0.11 - 0.059pH \quad (V, NHE) \quad (7)$$

therefore

$$\eta = -0.11 - E^0(A/A^-) - 0.059pH \quad (8)$$

The influence of pH on $E^0(A/A^-)$ was determined by differential-pulse polarography (Figure 7). Between pH 0 and 2, where both the oxidized and reduced forms of the cobaltocenedicarboxylic acid are protonated, the half-wave potential is constant and equal to -0.32 V (NHE). In the pH domain 2–5, the potential decreases linearly, the slope of the straight line being -0.10 V/pH.²¹ A slope of -0.12 V/pH is expected from the stoichiometry of reaction 9, during which two protons are consumed. Above pH 6, when



both the oxidized and reduced forms of cobaltocenedicarboxylic acid are fully deprotonated, and half-wave potential attains the constant value of -0.62 V (NHE). The occurrence of only one region of pH dependence with a single slope dE^0/dpH further confirms the equality of the first and the second dissociation constants of both oxidized and reduced cobaltocenedicarboxylic acid.

From the polarographic findings, the overvoltage for electron transfer from the TiO_2 conduction band to cobaltoceniumdicarboxylate should increase by 59 mV/pH at a pH below 3 and above 7. In the intermediate group, the overvoltage should increase with pH:

$$\eta = -0.11 - E^0(A/A^-, pH 0) - 0.059pH \quad (10)$$

(21) In the pH region 5–8 the polarographic wave splits into two waves (two maxima in the differential-pulse polarogram) as indicated by the lower lying points in Figure 7, which correspond to the electrode reaction (9) at more negative potential and the reaction $[Co(C_5H_4COO)_2]^{-} + e^{-} \rightarrow [Co(C_5H_4COO)_2]^{2-}$ at more positive potential, where the former gradually disappears at more alkaline pH.

where $E^\circ(A/A^-, \text{pH } 0)$ is the redox potential associated with reaction 9 extrapolated to pH 0. Combining (10) with (5) and (4) yields

$$\log k_2 = A - \alpha(\text{pH}) \quad (11)$$

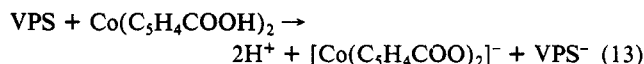
where $A = \log(4\pi r^2 N_A k_{\text{het}}^\circ) + \alpha F(0.11 + E^\circ(A/A^-, \text{pH } 0)/RT)$. Equation 11 predicts a linear relation between $\log k_2$ and pH with a slope of $-\alpha$. This is confirmed experimentally in Figure 5, where we find a linear decrease of $\log k_2$ with pH in the range $4 \lesssim \text{pH} \lesssim 10$. In this pH domain reaction 9 appears to be the kinetically favored reduction pathway. The value $\alpha = 0.5$ obtained indicates a symmetrical transition state for the electron-transfer reaction. We conclude that over a large pH domain the reduction of **1** by TiO_2 conduction band electrons involves simultaneous transfer of two protons to the reduced acceptor. In this context, recent flash photolysis results by Brown and Darwent²⁰ should be mentioned. These authors also noted the importance of acid-base equilibria in determining the rate of electron transfer from colloidal TiO_2 to methyl orange as an acceptor.

The kinetic analysis presented so far neglects Coulombic effects in the diffusional approach of semiconductor particle and acceptor. Therefore, eq 11 is strictly valid only when the acceptor and/or particle is uncharged or the ionic strength is high. To correct for variation in electrostatic attraction as the pH changes, Brown and Darwent²² introduce a relation of the type

$$\log k_2 = A - \left(\alpha + \frac{\beta}{I^{1/2}} \right) \text{pH} + \frac{\beta}{I^{1/2}} \text{PZZP} \quad (12)$$

where β is a constant that is negative for **1** as electron acceptor, I is the ionic strength, and PZZP is the point of zero ζ potential of the TiO_2 particles. From eq 12 it is seen that for low ionic strength the slope of the $d \log k_2 / d\text{pH}$ plot does not correspond straightforwardly to the transfer coefficient. Coulombic effects could play an important role in the reduction of a negative ion such as **1** by conduction band electrons of TiO_2 and this could provide an important clue to the understanding of the effect of pH on k_2 as shown in Figure 5. Further experimental work at various strength values is required to assess these effects.

It remains to be discussed why **1** in acidic solution enhances strongly the rate of interfacial electron transfer from the TiO_2 conduction band to electron acceptors, such as VPS. We note first that the simple sequence of reaction 9 followed by homogeneous electron transfer



cannot account for this observation. At 10^{-5} M concentration of **1** and pH 3.5 the mean formation time of $\text{Co}(\text{C}_5\text{H}_4\text{COOH})_2$ is 4 ms, which is much longer than $\tau = 8 \mu\text{s}$ obtained for electron transfer from TiO_2 particles to VPS under these conditions.

Using a dialysis method,²³ we found that a significant fraction (ca. 15%) of **1** is associated at pH 3.5 with the TiO_2 colloid. (At pH 10 the adsorption of **1** is negligibly small). Apparently, it is the adsorbed part of **1** that affords the electron-transfer catalysis. While at this time a detailed mechanism for this catalytic effect cannot be given, it is likely that electron traps at the particle surface (surface states) are eliminated through interaction with **1**. Another possibility is that **1** shifts cathodically the conduction band position of the TiO_2 particle by changing the potential drop in the Helmholtz layer.²⁴ We have attempted to produce a similar shift by adsorbing negatively charged ions (benzenesulfonate, benzoate, sulfate, etc.) on the particle surface, but none of these agents was found to affect the electron-transfer rate to VPS. Further studies are presently under way to investigate this unique and important effect.

Acknowledgment. This work was supported by the Swiss National Science Foundation and the Gas Research Institute, Chicago, IL (subcontract with the Solar Energy Research Institute, Golden, CO). A travel stipend from the Heinrich Hertz-Stiftung of the Ministry of Education, Düsseldorf, West Germany, to U.K. is gratefully acknowledged.

Registry No. **1**, 96453-13-3; TiO_2 , 13463-67-7; viologen propane-sulfonate, 77951-49-6.

(22) Brown, G. T.; Darwent, J. R. *J. Chem. Soc., Chem. Commun.*, in press. We thank Dr. Darwent for communicating to us these results prior to publication.

(23) Moser, J.; Grätzel, M. *J. Am. Chem. Soc.* **1984**, 106, 6557.

(24) We wish to thank Dr. J. R. Darwent, University of London, for suggesting this possibility to us.

(25) Recent EPR investigations of the electrons trapped in colloidal TiO_2 established that the blue color observed in acid solution is due to Ti^{3+} at the particle surface (Howe, R.; Grätzel, M., submitted for publication in *J. Phys. Chem.*).